Journal of The Electrochemical Society, **149** (3) A307-A318 (2002)
0013-4651/2002/149(3)/A307/12/$7.00 © The Electrochemical Society, Inc.

Estimation of Diffusion Coefficient of Lithium in Carbon Using AC Impedance Technique

Qingzhi Guo,* Venkat R. Subramanian, John W. Weidner,** and R. E. White***,z**

Center for Electrochemical Engineering, Department of Chemical Engineering, University of South Carolina, Columbia, South Carolina 29208, USA

The validity of estimating the solid phase diffusion coefficient, D_s, of a lithium intercalation electrode from impedance measurement by a modified electrochemical impedance spectroscopy (EIS) method is studied. A macroscopic porous electrode model and concentrated electrolyte theory are used to simulate the synthetic impedance data. The modified EIS method is applied for estimating D_s. The influence of parameters such as the exchange current density, radius of active material particle, solid phase conductivity, porosity, volume fraction of inert material, and thickness of the porous carbon intercalation electrode, the solution phase diffusion coefficient, and transference number, on the validity of D_s estimation, is evaluated. A simple dimensionless group is developed to correlate all the results. It shows that the accurate estimation of D_s requires large particle size, small electrode thickness, large solution diffusion coefficient, and low active material loading. Finally, a ''full model'' method is developed for the cases where the modified EIS method does not work well.
 [DOI: 10.1149/1.1447224]

Manuscript submitted August 2, 2001; revised manuscript received October 10, 2001. Available electronically February 5, 2002.

The transport phenomena inside a battery have been attracting a lot of attention. Accurate measurement of parameters such as diffusion coefficients in both the solution phase and the solid phase of a battery can help in understanding what is occurring inside it and ways to improve its performance. The extraction of solid phase diffusion coefficient, D_s, of an intercalation electrode in a lithium-ion battery from ac impedance measurement is of great interest to us.[1-6] Basically, the impedance data from either the semi-infinite diffusion region or the transition region of the Nyquist plots are used to estimate this parameter.

Among the methods developed to estimate D_s of a lithium-ion electrode, the Yu *et al.* modified electrochemical impedance spectroscopy (EIS) method[6] seems to be very useful. It was an extension of the Haran *et al.* model[7] of a metal hydride electrode for alkaline batteries. Both models are based on the assumption that there is no solution diffusion limitation inside the working porous electrode pellet and each spherical active material particle behaves identically and has the same reaction current density on its surface. One advantage of the Yu *et al.* model, compared to other approaches such as traditional Warburg approach, potential intermittent titration technique (PITT) and galvanostatic intermittent titration technique (GITT), is that we are not required to know exactly the parameters such as the steady-state lithium-ion concentration, c_0, surface concentration, c_s, of intercalation species lithium on the solid particle, open-circuit potential (OCP) gradient dU/dx inside the porous electrode, molar volume, V_m, of the lithiated material, and effective surface area per unit mass ''A'' of the porous electrode.[8-11] Another advantage, compared to the traditional Warburg approach, is that the impedance data with even lower frequency, which are supposed to be dominated even more likely by the solid phase diffusion, are used for the estimation of D_s. It is easy to realize this by the fact that the traditional Warburg approach uses the impedance data with gradient or slope in the Nyquist plot equal to -1 and the modified EIS method uses the data with gradient more negative than -1.5, which has even lower frequency.

The Yu *et al.* model has limitation here. We have no assurance that there is large difference between the values of solution phase diffusion coefficient, D, and solid phase diffusion coefficient, D_s. As a result, the ignorance of solution phase diffusion limitation might be a problem. Furthermore, porous electrodes tend to make the reaction current nonuniformly distributed due to unmatched potential drop in both solution and solid phase caused by their different conductivity. Hence, the validity of the estimation of D_s in the lab by the Yu *et al.* work is not guaranteed.

Doyle *et al.*[12] investigated the possibility of estimating the parameter D_s from the impedance response of a commercial lithium-polymer cell, which consists of a porous intercalation positive electrode $LiTiS_2$ and a lithium foil negative electrode. They showed that only when the true value of solid phase diffusion coefficient of an intercalation electrode is small enough, *i.e.*, less than 10^{-13} cm^2/s for the $LiTiS_2$ electrode in their work, they could get a relatively reliable estimation of this parameter from the impedance data of a full commercial cell using the existing methods in the literature. They concluded that the low frequency spectrum needs to be dominated by diffusion impedance in the solid phase if a valid estimation of D_s is desired. The value of 10^{-13} cm^2/s of D_s of the $LiTiS_2$ electrode seems to be the threshold order of magnitude for such domination in their case. Even though they were estimating D_s from the impedance response of a full cell instead of a working electrode, their result is still persuasive since the contribution to the total impedance from the separator and counter electrode region combined is negligible in the low frequency region, compared to that from the working electrode. This is seen from Fig. 3 of their work. Unfortunately, they did not discuss in their work what we could do in order to get a reliable estimation of D_s assuming the true value of D_s to be around 10^{-10} cm^2/s or higher, the order of magnitude for lithium intercalation electrode often referred in literature. In this communication, our objective is to find out the experimental conditions under which we can safely estimate the D_s of lithium in a carbon electrode from ac impedance by using the modified EIS model of Yu *et al.*[6] For the case where this method is bad for the estimation, an alternate method is provided and discussed. A Swagelok T-cell structure consisting of porous carbon intercalation working electrode, one lithium foil counter electrode, and one lithium foil reference electrode is considered (Fig. 1). This figure is similar to Fig. 1 in Ref. 6 except that we treat the working electrode as the superposition of two continua, one representing the solution and the other representing the solid matrix, instead of as an assembly of identically behaved spherical particles. The procedure in our study is first, we solve the model equations based on the macroscopic porous electrode theory and concentrated electrolyte theory for the T-cell to generate synthetic impedance data; then, we apply the modified EIS method to extract the value of D_s from these data. And then, we are able to evaluate the accuracy of estimation by comparing the estimated

* Electrochemical Society Student Member.
** Electrochemical Society Active Member.
*** Electrochemical Society Fellow.
z E-mail: white@engr.sc.edu

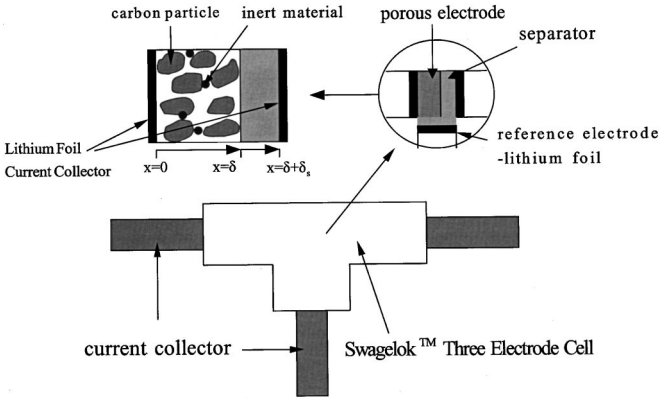

Figure 1. Schematic graph of a T-cell consisting of a carbon porous electrode.

value of D_s with the true parameter value we give as input in our model equations for the impedance simulation. In this work, the effect of some parameters, such as the exchange current density, i_0, solid phase conductivity, σ, thickness δ, active material particle size, R_s, porosity ε, and volume fraction of inert material, ε_{inert} (filler plus conducting material) of a porous carbon electrode, solution phase diffusion coefficient, D, and lithium-ion transference number, t_+^0, on the reliability of D_s estimation is studied. The impedance response of the working electrode in reference to a lithium foil adjacent to the interface of the working electrode and separator is used for the extraction of D_s.

According to Haran *et al.*,[7] the faradaic impedance of an electrode with the intercalation material particle of spherical shape is written as

$$Z(\omega) = \frac{\partial \eta_{R_s}}{\partial I} + \frac{(1-j)\sigma_0}{\sqrt{\omega}\left[\coth(1+j)\sqrt{\frac{\omega R_s^2}{2D_s}} - (1-j)\sqrt{\frac{D_s}{2\omega R_s^2}}\right]^{1/2}} \quad [1]$$

where η_{Rs} is the overpotential at the particle surface (radius $r = R_s$), I is the reaction current on the surface, j is the imaginary number, $\sqrt{-1}$, and σ_0 is the modified Warburg prefactor expressed as

$$\sigma_0 = \frac{\partial J/\partial c_s}{\partial J/\partial \eta_{R_s}} \times \frac{m}{aV(1-\varepsilon)F\sqrt{2D_s}} \quad [2]$$

where V is the volume of the working pellet electrode, J is the specific current per unit mass of active material, m is the mass of active material, and a is the surface area per unit volume of the electrode. After separating the impedance of expression 1 into the real part Z_{Re} and the imaginary part Z_{Im}, one gets the gradient of the impedance curve in the transition region of the Nyquist plot (see Fig. 9 of Ref. 6)

$$\frac{dZ_{Im}}{dZ_{Re}} = \frac{(S_3S_5 + S_4S_7 - S_1S_6 + S_2S_8)T_4 - 2T_3(S_4S_3 + S_2S_1)}{(S_3S_6 - S_4S_8 + S_1S_5 + S_2S_7)T_4 - 2T_5(S_4S_3 + S_2S_1)} \quad [3]$$

where

$$T_3 = (S_4S_5 - S_2S_6); \quad T_4 = (S_4^2 + S_2^2); \quad T_5 = (S_4S_6 + S_2S_5) \quad [4]$$

and

$$S_1 = S_5S_6$$
$$S_2 = 2\Psi - S_5$$
$$S_3 = 2\coth(\Psi)\cot(\Psi)(1 - \Psi S_6) - 2\Psi S_5 + S_8$$
$$S_4 = 2\Psi\coth(\Psi)\cot(\Psi) - S_6$$
$$S_5 = \coth(\Psi) - \cot(\Psi)$$
$$S_6 = \coth(\Psi) + \cot(\Psi)$$
$$S_7 = 2 - S_1$$
$$S_8 = \cot(\Psi)^2 + \coth(\Psi) \quad [5]$$

where

$$\Psi = R_s\sqrt{\frac{\omega}{2D_s}} \quad [6]$$

In our work, the gradient at each available impedance data point in the transition region is calculated numerically by

$$\frac{dZ_{Im}}{dZ_{Re}} = \frac{Z_{Im}(\omega + \Delta\omega) - Z_{Im}(\omega - \Delta\omega)}{Z_{Re}(\omega + \Delta\omega) - Z_{Re}(\omega - \Delta\omega)} \quad [7]$$

This numerical calculation of the gradient works satisfactorily here, since we have as many as 100 points per decade of frequency in our simulation. Next, we can either use a nonlinear parameter estimation technique to get the estimation of D_s from the calculated impedance gradient data or determine the value of Ψ at each available data point and then obtain D_s by substitution into expression 6 of the frequency value at that point and the radius of solid particles. Finally, the validity of the estimation of D_s is evaluated by the accuracy of estimation

$$\text{Accuracy} = \frac{\text{estimated value of } D_s}{\text{true value of } D_s} \times 100\% \quad [8]$$

In this work, a carbon intercalation electrode with 50% state-of-charge is considered.

Mathematical Model

The model equations used in this pseudo-two-dimensional model for the Swagelok T-cell, one-dimensional with respect to spatial direction x, and pseudo-second dimensional with respect to radial direction inside each spherical particle, are similar to those used by Doyle *et al.*[12]

Conservation of charge in the porous carbon electrode is given by

$$aFj_{n,f} = \frac{\partial i_2}{\partial x} - aC_{dl}\frac{\partial(\Phi_1 - \Phi_2)}{\partial t} \quad [9]$$

with the assumption that the double-layer capacitance c_{dl} is constant and independent of the solution phase concentration and potential.[12]

Equation 10 is used to account for the material balance in the solution phase

$$\frac{\partial(\varepsilon c)}{\partial t} = \frac{\partial}{\partial x}\left(\varepsilon D_{eff}\frac{\partial c}{\partial x}\right) - \frac{i_2}{F}\frac{\partial t_+^0}{\partial x} + aj_{n,f}(1 - t_+^0) + \frac{aC_{dl}}{F}t_-^0\frac{\partial(\Phi_1 - \Phi_2)}{\partial t} \quad [10]$$

where the effective diffusion coefficient, D_{eff}, is related to the bulk solution diffusion coefficient, D, by expression 11 to account for tortuosity of diffusion path inside the electrode

$$D_{\text{eff}} = \varepsilon^{0.5} D \quad [11]$$

Application of Ohm's law in the solid phase and solution phase yields

$$I - i_2 = -\sigma_{\text{eff}} \frac{\partial \Phi_1}{\partial x} \quad [12]$$

$$i_2 = -\kappa_{\text{eff}} \frac{\partial \Phi_2}{\partial x} + \frac{2\kappa_{\text{eff}} RT}{F}\left(1 + \frac{d \ln f_{\pm}}{d \ln c}\right)(1 - t_+^0) \frac{\partial \ln c}{\partial x} \quad [13]$$

where the solid phase effective conductivity, σ_{eff}, and the solution phase effective conductivity, κ_{eff}, are related to bulk solid conductivity σ and bulk solution conductivity κ by expressions

$$\sigma_{\text{eff}} = (1 - \varepsilon)^{1.5} \sigma \quad [14]$$

$$\kappa_{\text{eff}} = \varepsilon^{1.5} \kappa \quad [15]$$

to account for the actual path of the conducting species.[13]

The electrode kinetics relationship is assumed to follow a simple Butler-Volmer equation, Eq. 16. The electrochemical reaction on the carbon particle surface is given elsewhere[6]

$$j_{\text{n,f}} F = i_0\left(\exp\left[\frac{\alpha_a F}{RT}(\Phi_1 - \Phi_2 - U)\right] - \exp\left[-\frac{\alpha_c F}{RT}(\Phi_1 - \Phi_2 - U)\right]\right) \quad [16]$$

In Eq. 16, the equilibrium potential, U, is fitted from the experimental data[14] by

$$U = -0.16 + 1.32 \exp\left(-3.0\frac{c_s}{c_t}\right) + 10.0 \exp\left(-2000.0\frac{c_s}{c_t}\right) \quad [17]$$

where the surface concentration, c_s of the active material carbon particle is related to Eq. 18, which describes the solid phase diffusion of Li in the spherical carbon particle, and its boundary conditions 19 and 20

$$\frac{\partial c_s}{\partial t} = D_s\left(\frac{\partial^2 c_s}{\partial r^2} + \frac{2}{r}\frac{\partial c_s}{\partial r}\right) \quad [18]$$

$$-D_s \frac{\partial c_s}{\partial r} = 0 \quad \text{at} \quad r = 0 \quad [19]$$

$$-D_s \frac{\partial c_s}{\partial r} = j_{\text{n,f}} \quad \text{at} \quad r = R_s \quad [20]$$

For the separator region, material balance leads to

$$\frac{\partial(\varepsilon c)}{\partial t} = \frac{\partial}{\partial x}\left(\varepsilon D_{\text{eff}} \frac{\partial c}{\partial x}\right) - \frac{i_2}{F}\frac{\partial t_+^0}{\partial x} \quad [21]$$

and Ohm's law leads to the same form of equation as Eq. 13 except that the solution phase current density i_2 is equal to the total current density I, which does not change with x.

For the counter electrode, a similar form of Butler-Volmer equation to that of Eq. 16 is also assumed. Then, we have Eq. 22 for the counter lithium foil electrode after the consideration of double layer charging and discharging

$$-I = i_{0,c}\left(\exp\left[\frac{\alpha_a F}{RT}(\Phi_1 - \Phi_2 - U_c)\right] - \exp\left[-\frac{\alpha_c F}{RT}(\Phi_1 - \Phi_2 - U_c)\right]\right) + C_{\text{dl,c}} \frac{\partial(\Phi_1 - \Phi_2)}{\partial t} \quad [22]$$

The local equilibrium potential of the counter electrode is zero, independent of the activity of Li or Li^+, in reference to a lithium foil electrode

$$U_c = 0 \quad [23]$$

After a similar mathematical treatment of the above equations to that of the Doyle *et al.* work,[12] finally we have the following equations in the frequency domain

$$\varepsilon\omega\tilde{c}_{\text{Re}} = \varepsilon D_{\text{eff}} \frac{\partial^2 \tilde{c}_{\text{Im}}}{\partial x^2} + a\tilde{j}_{\text{n,f,Im}}(1 - t_+^0) + \frac{aC_{\text{dl}}}{F}\omega t_-^0[\tilde{\Phi}_{1,\text{Re}} - \tilde{\Phi}_{2,\text{Re}}] \quad [24]$$

$$-\varepsilon\omega\tilde{c}_{\text{Im}} = \varepsilon D_{\text{eff}} \frac{\partial^2 \tilde{c}_{\text{Re}}}{\partial x^2} + a\tilde{j}_{\text{n,f,Re}}(1 - t_+^0) - \frac{aC_{\text{dl}}}{F}\omega t_-^0[\tilde{\Phi}_{1,\text{Im}} - \tilde{\Phi}_{2,\text{Im}}] \quad [25]$$

$$aF\tilde{j}_{\text{n,f,Re}} = \sigma_{\text{eff}} \frac{\partial^2 \tilde{\Phi}_{1,\text{Re}}}{\partial x^2} + a\omega C_{\text{dl}}[\tilde{\Phi}_{1,\text{Im}} - \tilde{\Phi}_{2,\text{Im}}] \quad [26]$$

$$aF\tilde{j}_{\text{n,f,Im}} = \sigma_{\text{eff}} \frac{\partial^2 \tilde{\Phi}_{1,\text{Im}}}{\partial x^2} - a\omega C_{\text{dl}}[\tilde{\Phi}_{1,\text{Re}} - \tilde{\Phi}_{2,\text{Re}}] \quad [27]$$

$$\sigma_{\text{eff}} \frac{\partial^2 \tilde{\Phi}_{1,\text{Re}}}{\partial x^2} = -\kappa_{\text{eff}} \frac{\partial^2 \tilde{\Phi}_{2,\text{Re}}}{\partial x^2} + \frac{2\kappa_{\text{eff}} RT}{F}\left(\frac{1}{c_0} + \frac{f'_{\pm,0}}{f_{\pm,0}}\right) \times (1 - t_+^0) \frac{\partial^2 \tilde{c}_{\text{Re}}}{\partial x^2} \quad [28]$$

$$\sigma_{\text{eff}} \frac{\partial^2 \tilde{\Phi}_{1,\text{Im}}}{\partial x^2} = -\kappa_{\text{eff}} \frac{\partial^2 \tilde{\Phi}_{2,\text{Im}}}{\partial x^2} + \frac{2\kappa_{\text{eff}} RT}{F}\left(\frac{1}{c_0} + \frac{f'_{\pm,0}}{f_{\pm,0}}\right) \times (1 - t_+^0) \frac{\partial^2 \tilde{c}_{\text{Im}}}{\partial x^2} \quad [29]$$

$$-\varepsilon\omega\tilde{c}_{\text{Im}} = \varepsilon D_{\text{eff}} \frac{\partial^2 \tilde{c}_{\text{Re}}}{\partial x^2} \quad [30]$$

$$\varepsilon\omega\tilde{c}_{\text{Re}} = \varepsilon D_{\text{eff}} \frac{\partial^2 \tilde{c}_{\text{Im}}}{\partial x^2} \quad [31]$$

$$0 = -\kappa_{\text{eff}} \frac{\partial^2 \tilde{\Phi}_{2,\text{Re}}}{\partial x^2} + \frac{2\kappa_{\text{eff}} RT}{F}\left(\frac{1}{c_0} + \frac{f'_{\pm,0}}{f_{\pm,0}}\right)(1 - t_+^0) \frac{\partial^2 \tilde{c}_{\text{Re}}}{\partial x^2} \quad [32]$$

$$0 = -\kappa_{\text{eff}} \frac{\partial^2 \tilde{\Phi}_{2,\text{Im}}}{\partial x^2} + \frac{2\kappa_{\text{eff}} RT}{F}\left(\frac{1}{c_0} + \frac{f'_{\pm,0}}{f_{\pm,0}}\right)(1 - t_+^0) \frac{\partial^2 \tilde{c}_{\text{Im}}}{\partial x^2} \quad [33]$$

where Eq. 24-29 are used for the porous electrode and Eq. 30-33 for the separator. Note that $\tilde{j}_{\text{n,f,Re}}$ and $\tilde{j}_{\text{n,f,Im}}$ that appeared in Eq. 24-27 are related to $\tilde{\Phi}_{1,\text{Re}}, \tilde{\Phi}_{1,\text{Im}}, \tilde{\Phi}_{2,\text{Re}}$, and $\tilde{\Phi}_{2,\text{Im}}$ by Eq. A-1 to A-8.

The boundary conditions for the above Eq. 24-33 are tabulated in Table I.

Table I. The boundary conditions for the governing equations in frequency domain. We set $I = 1\ \mathrm{A/cm^2}$ in our work for convenience.

Boundary conditions		
$-\varepsilon^{1.5} D \left.\frac{\partial \tilde{c}_{\mathrm{Re}}}{\partial x}\right\|_{x=0+} = 0$	$-\varepsilon^{1.5} D \left.\frac{\partial \tilde{c}_{\mathrm{Re}}}{\partial x}\right\|_{x=\delta-} = -\varepsilon_s^{1.5} D \left.\frac{\partial \tilde{c}_{\mathrm{Re}}}{\partial x}\right\|_{x=\delta+}$	$-\varepsilon_s^{1.5} D \left.\frac{\partial \tilde{c}_{\mathrm{Re}}}{\partial x}\right\|_{x=(\delta+\delta_s)-} = \frac{It^0}{F}$
$-\varepsilon^{1.5} D \left.\frac{\partial \tilde{c}_{\mathrm{Im}}}{\partial x}\right\|_{x=0+} = 0$	$-\varepsilon^{1.5} D \left.\frac{\partial \tilde{c}_{\mathrm{Im}}}{\partial x}\right\|_{x=\delta-} = -\varepsilon_s^{1.5} D \left.\frac{\partial \tilde{c}_{\mathrm{Im}}}{\partial x}\right\|_{x=\delta+}$	$-\varepsilon_s^{1.5} D \left.\frac{\partial \tilde{c}_{\mathrm{Im}}}{\partial x}\right\|_{x=(\delta+\delta_s)-} = 0$
$-(1-\varepsilon)^{1.5}\sigma \left.\frac{\partial \tilde{\Phi}_{1,\mathrm{Re}}}{\partial x}\right\|_{x=0+} = I$	$-(1-\varepsilon)^{1.5}\sigma \left.\frac{\partial \tilde{\Phi}_{1,\mathrm{Re}}}{\partial x}\right\|_{x=\delta+} = 0$	$\tilde{\Phi}_{1,\mathrm{Re}}\|_{x=(\delta+\delta_s)-} = 0$
$-(1-\varepsilon)^{1.5}\sigma \left.\frac{\partial \tilde{\Phi}_{1,\mathrm{Im}}}{\partial x}\right\|_{x=0+} = 0$	$-(1-\varepsilon)^{1.5}\sigma \left.\frac{\partial \tilde{\Phi}_{1,\mathrm{Im}}}{\partial x}\right\|_{x=\delta+} = 0$	$\tilde{\Phi}_{1,\mathrm{Im}}\|_{x=(\delta+\delta_s)-} = 0$
$-\varepsilon^{1.5}\kappa \left.\frac{\partial \tilde{\Phi}_{2,\mathrm{Re}}}{\partial x}\right\|_{x=0+} = 0$	$-\varepsilon^{1.5}\kappa \left.\frac{\partial \tilde{\Phi}_{2,\mathrm{Re}}}{\partial x}\right\|_{x=\delta-} = -\varepsilon_s^{1.5}\kappa \left.\frac{\partial \tilde{\Phi}_{2,\mathrm{Re}}}{\partial x}\right\|_{x=\delta+}$	$-I = \frac{i_{0,c}F}{RT}(\tilde{\Phi}_{1,\mathrm{Re}} - \tilde{\Phi}_{2,\mathrm{Re}})\|_{x=(\delta+\delta_s)-} - C_{\mathrm{dl,c}}\omega(\tilde{\Phi}_{1,\mathrm{Im}} - \tilde{\Phi}_{2,\mathrm{Im}})\|_{x=(\delta+\delta_s)-}$
$-\varepsilon^{1.5}\kappa \left.\frac{\partial \tilde{\Phi}_{2,\mathrm{Im}}}{\partial x}\right\|_{x=0+} = 0$	$-\varepsilon^{1.5}\kappa \left.\frac{\partial \tilde{\Phi}_{2,\mathrm{Im}}}{\partial x}\right\|_{x=\delta-} = -\varepsilon_s^{1.5}\kappa \left.\frac{\partial \tilde{\Phi}_{2,\mathrm{Im}}}{\partial x}\right\|_{x=\delta+}$	$0 = \frac{i_{0,c}F}{RT}(\tilde{\Phi}_{1,\mathrm{Im}} - \tilde{\Phi}_{2,\mathrm{Im}})\|_{x=(\delta+\delta_s)-} + C_{\mathrm{dl,c}}\omega(\tilde{\Phi}_{1,\mathrm{Re}} - \tilde{\Phi}_{2,\mathrm{Re}})\|_{x=(\delta+\delta_s)-}$

The real and imaginary parts of impedance of the working electrode are given by

$$Z_{\mathrm{Re}} = \tilde{\Phi}_{1,\mathrm{Re}}|_{x=0+} - \tilde{\Phi}_{1,\mathrm{Re}}|_{x=\delta-}$$

and

$$Z_{\mathrm{Im}} = \tilde{\Phi}_{1,\mathrm{Im}}|_{x=0+} - \tilde{\Phi}_{1,\mathrm{Im}}|_{x=\delta-} \quad [34]$$

In this work, we treat the total perturbation current, I, as the input perturbation signal with purely real unity value.

Numerical Solution

We use a numerical algebraic equation package of FORTRAN called General Nonlinear Equation Solver (GNES) to solve the above linear equations Eq. 24-33. This solver has the same calling protocol as that of the differential equation solver called DASSL. As was already demonstrated in Fig. 11-14 of Ref. 14, a sharp profile of concentration and potential exists at the interfaces of the porous electrode and separator, and the separator and lithium foil electrode. In order to resolve the impedance response more appropriately in our work, especially in the high frequency limit, we discretize unevenly the thickness of the porous electrode as well as that of the separator region. In this work, dense node points are applied to the regions adjacent to the interfaces between the porous electrode and separator and between the separator and counter electrode. To transform the differential equations Eq. 24-33 to the algebraic ones, we approximate the derivatives of each dependent variable by using three-point finite difference method. Finally, the solution vector **Y** is found by evaluating the residual vector **DELTA**

$$\mathbf{DELTA} = \mathbf{G}(\mathbf{X}, \mathbf{Y}) \quad [35]$$

where $\mathbf{G}(\mathbf{X}, \mathbf{Y})$ is the governing equation vector in the residual form. **Y** has the structure of

$$\mathbf{Y} = \begin{bmatrix} \tilde{c}_{\mathrm{Re}}[1],\ \tilde{c}_{\mathrm{Im}}[1],\ \tilde{\Phi}_{1,\mathrm{Re}}[1],\ \tilde{\Phi}_{1,\mathrm{Im}}[1],\ \tilde{\Phi}_{2,\mathrm{Re}}[1],\ \tilde{\Phi}_{2,\mathrm{Im}}[1],\ \ldots \\ \tilde{c}_{\mathrm{Re}}[i],\ \tilde{c}_{\mathrm{Im}}[\mathrm{i}],\ \tilde{\Phi}_{1,\mathrm{Re}}[\mathrm{i}],\ \tilde{\Phi}_{1,\mathrm{Im}}[i],\ \tilde{\Phi}_{2,\mathrm{Re}}[i],\ \tilde{\Phi}_{2,\mathrm{Im}}[i],\ \ldots \\ \tilde{c}_{\mathrm{Re}}[N],\ \tilde{c}_{\mathrm{Im}}[\mathrm{N}],\ \tilde{\Phi}_{1,\mathrm{Re}}[\mathrm{N}],\ \tilde{\Phi}_{1,\mathrm{Im}}[\mathrm{N}],\ \tilde{\Phi}_{2,\mathrm{Re}}[\mathrm{N}],\ \tilde{\Phi}_{2,\mathrm{Im}}[\mathrm{N}] \\ \tilde{c}_{\mathrm{Re}}[N+1],\ \tilde{c}_{\mathrm{Im}}[\mathrm{N}+1],\ \tilde{\Phi}_{2,\mathrm{Re}}[\mathrm{N}+1],\ \tilde{\Phi}_{2,\mathrm{Im}}[\mathrm{N}+1],\ \ldots \\ \tilde{c}_{\mathrm{Re}}[N+i],\ \tilde{c}_{\mathrm{Im}}[\mathrm{N}+\mathrm{i}],\ \tilde{\Phi}_{2,\mathrm{Re}}[\mathrm{N}+i],\ \tilde{\Phi}_{2,\mathrm{Im}}[\mathrm{N}+i],\ \ldots \\ \tilde{c}_{\mathrm{Re}}[M-1],\ \tilde{c}_{\mathrm{Im}}[\mathrm{M}-1],\ \tilde{\Phi}_{2,\mathrm{Re}}[\mathrm{M}-1],\ \tilde{\Phi}_{2,\mathrm{Im}}[\mathrm{M}-1] \\ \tilde{c}_{\mathrm{Re}}[M],\ \tilde{c}_{\mathrm{Im}}[\mathrm{M}],\ \tilde{\Phi}_{1,\mathrm{Re}}[\mathrm{M}],\ \tilde{\Phi}_{1,\mathrm{Im}}[\mathrm{M}],\ \tilde{\Phi}_{2,\mathrm{Re}}[\mathrm{M}],\ \tilde{\Phi}_{2,\mathrm{Im}}[\mathrm{M}] \end{bmatrix} \quad [36]$$

The impedance of the whole cell can be obtained by

$$Z_{\mathrm{Re}} = \tilde{\Phi}_{1,\mathrm{Re}}[1] - \tilde{\Phi}_{1,\mathrm{Re}}[\mathrm{M}] \ \text{ and } \ Z_{\mathrm{Im}} = \tilde{\Phi}_{1,\mathrm{Im}}[1] - \tilde{\Phi}_{1,\mathrm{Im}}[\mathrm{M}] \quad [37]$$

and the impedance of the porous electrode in reference to a lithium foil electrode at the interface of the porous electrode and separator is given by

Table II. The values for all the parameters used in this model under base conditions.

Parameter	Carbon electrode	Separator	Li foil	Reference
D_s (cm^2/s)	3.9×10^{-10}			11
D (cm^2/s)		7.5×10^{-7}		11
t_+^0		0.363		11
κ (S/cm)		2.6×10^{-3}		11
c_t (mol/cm^3)	0.02639			11
c_s (mol/cm^3)	0.0139867			11
ε	0.357			11
ε_s		0.724		11
ε_{inert}	0.172			11
C_{dl} (F/cm^2)	10^{-5}			Assumed
$C_{dl,c}$ (F/cm^2)			10^{-5}	Assumed
i_0 (mA/cm^2)	0.11			11
$i_{0,c}$ (mA/cm^2)			1.26	9
σ (S/cm)	1.0			11
$f'_{\pm,0}$		0		Assumed
c_0 (mol/cm^3)		0.001		Assumed
R_s (cm)	0.00125			11
δ (cm)	0.01			11
δ_s (cm)		0.0052		11
T (K)	298.15			Assumed

$$Z_{Re} = \tilde{\Phi}_{1,Re}[1] - \tilde{\Phi}_{2,Re}[N] \quad \text{and} \quad Z_{Im} = \tilde{\Phi}_{1,Im}[1] - \tilde{\Phi}_{2,Im}[N] \qquad [38]$$

Results and Discussion

The base values of all the parameters used for the T-cell system under consideration are tabulated in Table II. A demonstration of the simulated impedance response of the full T-cell, as well as the contribution to the full cell impedance from each region, with base parameter values put in the model equations described above is seen in Fig. 2. The high frequency loop of the full cell impedance curve is overlapped by two semicircles. The appearance of first impedance maximum is caused by the relative combined domination of impedance of the counter electrode and separator region. The second maximum is caused by the relative domination of the impedance from the porous carbon electrode. One can realize this by looking at the difference among the high frequency impedance loops simulated by using different parameter values of the exchange current density of both the porous and counter electrodes.

Parameter estimation by the modified EIS method.—Given the values of all the parameters, we are able to generate, by solving the model equations Eq. 24-33, a set of simulated impedance data over a wide range of frequency. The transition region of the Nyquist plot of the simulated impedance data can be used to get D_s back by the modified EIS method. We assume that the synthetic impedance data generated by solving the model equations for the T-cell in this work are "real" enough to represent the actual impedance behavior of such cell in the lab. As a result, the validity of applying the modified EIS method to the estimation of D_s in a carbon electrode can be evaluated after comparing the estimated value with the true value of D_s that we put in our model equations.

To start with, we have to justify which section of the transition region should be used for the estimation of D_s with a desired accuracy. The accuracy of estimation of D_s (for several different true values of D_s while keeping all the other parameters to their base values) from the impedance data in the transition region of Nyquist plot with the gradient ranging from -1.5 to -15 is given in Fig. 3 as a function of gradient. Maple's fsolve is used here. We observe that the accuracy is better when the gradient is more negative than -4.0, compared to the region, from -1.5 to -2.5, adopted by Yu *et al.*[6] However, data points with gradient more negative than -12.0 are likely to involve large error due to the round-of error caused by small change of the real part of impedance. Therefore, the transition region with gradient ranging from -4.0 to -12.0 is used in this work for the estimation of D_s. We also find that it is feasible to get a reliable estimation of D_s by using the modified EIS method when the true value of this parameter is less than 3.9×10^{-10} cm^2/s. One needs to know that assigning different base values other parameters, such as kinetics, from the ones in Table II might change the range of validity of D_s estimation. Thus, a thorough investigation of the influence of all the other parameters relevant to the validity of the estimation of D_s is needed. We expect to lead to an instructive

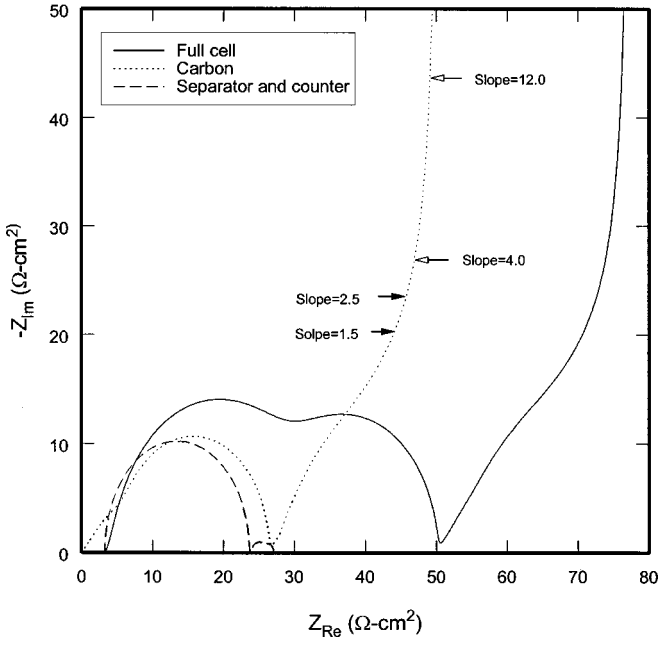

Figure 2. Demonstration of the simulated impedance response of a T-cell with base parameter values.

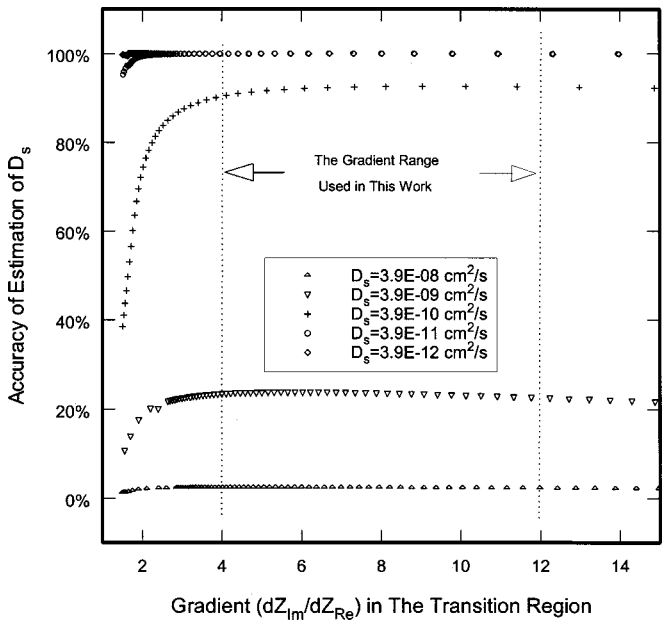

Figure 3. The accuracy of estimation of D_s as a function of the impedance gradient in the transition region (all the other parameters keep their base values).

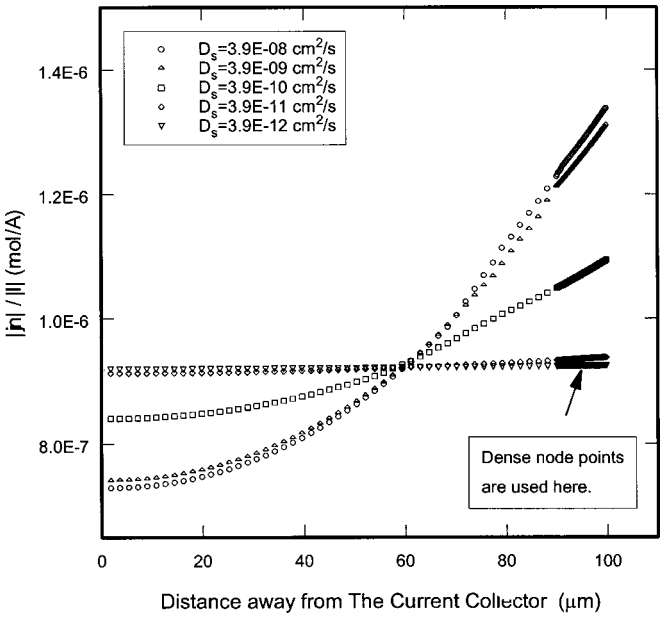

Figure 4. Comparison of reaction current distributions on the surface of carbon particle for different parameter values of D_s (all the other unmentioned parameters use their base values).

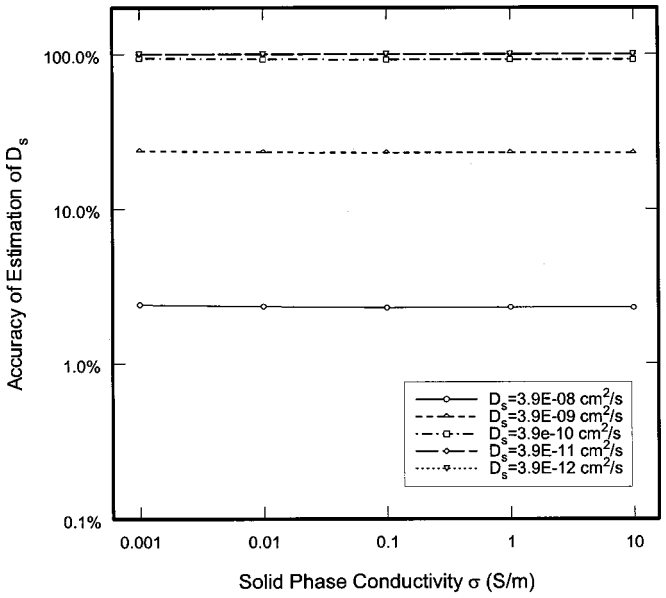

Figure 5. The accuracy of estimation of D_s with different parameter values of the solid phase conductivity (all the other unmentioned parameters keep their base value).

conclusion that helps us get a reliable estimation of D_s from real impedance data collected in the lab.

A nonlinear parameter estimation technique called Gauss-Newton method[15,16] is employed to get D_s back from the simulated impedance response of the working electrode in the remaining part of this work. The algorithm of this technique for the modified EIS method involves the following steps: First, assume initial guesses for the parameter vector **b**, which actually has only one element D_s in this case. Then, evaluate the Jacobian matrix **J** from Eq. 3, 4, 5, and 6. Next, use Eq. 39 to obtain the correction parameter vector $\Delta\mathbf{b}$

$$\Delta\mathbf{b} = (\mathbf{J}^{\mathrm{T}}\mathbf{J})^{-1}\mathbf{J}^{\mathrm{T}}(\mathbf{Y}^{*} - \mathbf{Y}) \qquad [39]$$

where $\mathbf{Y}^{*}$ and **Y** are the objective function vector with experimental and estimated values, respectively. After this, a new estimate of the parameter vector is evaluated from Eq. 40

$$\mathbf{b}^{(m+1)} = \mathbf{b}^{(m)} + \Delta\mathbf{b}^{(m)} \qquad [40]$$

where m is the number of corrections done. The estimation of D_s converges successfully to a value when the correction vector $\Delta\mathbf{b}$ becomes very small.

As stated before, for the modified EIS method to work well, the surface of each spherical particle in the porous electrode should have uniform reaction current distribution. Figure 4 demonstrates this, where a nonlinear reaction current inside the porous electrode exists for the true value of D_s greater than 3.9×10^{-10} cm^2/s. The characteristics of a porous electrode tend to make this current nonuniformly distributed. In order to use safely the modified EIS method, we need to make sure that the uniform reaction current distribution on each particle surface is present.

Through a simplified porous electrode model, Newman[17] derived two dimensionless groups, the dimensionless current density Eq. 41 and the dimensionless exchange current density Eq. 42, that could be used to judge the uniformity of the reaction current distribution inside the porous electrode.

$$\Delta = \frac{\alpha_a F I \delta}{RT}\left(\frac{1}{\kappa_{\mathrm{eff}}} + \frac{1}{\sigma_{\mathrm{eff}}}\right) \qquad [41]$$

$$\gamma^2 = (\alpha_a + \alpha_c)\frac{F a i_0 \delta^2}{RT}\left(\frac{1}{\kappa_{\mathrm{eff}}} + \frac{1}{\sigma_{\mathrm{eff}}}\right) \qquad [42]$$

In the above two expressions, Δ and γ^2 are ratios of the competing effects of the ohmic potential drop and slow electrode kinetics. For large values of either Δ or γ^2, the ohmic effect dominates, and as a result, the reaction distribution is nonuniform. For small values of both Δ and γ^2, the reaction distribution is more uniform. In our work, the importance of such parameters as the exchange current density i_0, thickness δ and specific surface area per unit volume a of the porous electrode to the valid estimation of solid phase diffusion coefficient is investigated. Since Newman's simple model does not consider solution diffusion limitation, the effect of the solution diffusion coefficient on the validity of estimation of D_s is also discussed in this paper. The superimposition of both solution phase diffusion and solid phase diffusion is believed to be present in the diffusion region of the impedance plot.[12] Besides, the influence of the transference number of lithium ion is also considered. Because the specific surface area a is related to the radius of the active material particle R_s, the porosity ε, and volume fraction of inert material $\varepsilon_{\mathrm{inert}}$ of the porous electrode by expression 43 for the spherical particle geometry, the change of a can only be made by changing one or some of the three parameters R_s, ε, and $\varepsilon_{\mathrm{inert}}$. Separate discussion on each of these parameters is carried out in this work

$$a = \frac{3}{R_s}(1 - \varepsilon - \varepsilon_{\mathrm{inert}}) \qquad [43]$$

Newman also pointed out that the reaction current in a porous electrode is somewhat more uniform as the value of solid phase effective conductivity and solution phase effective conductivity approach each other. By changing the solid phase conductivity, σ, and holding the solution phase conductivity, κ, constant, we can check the validity of D_s estimation.

Figure 5 shows that the change of solid phase conductivity has no apparent effect on the estimation accuracy when $\sigma \geqslant 0.001$ S/cm, $\sigma_{\mathrm{eff}} \geqslant \kappa_{\mathrm{eff}}$ in this case, by the modified EIS method over the true D_s range under study here. Thus, the accuracy of

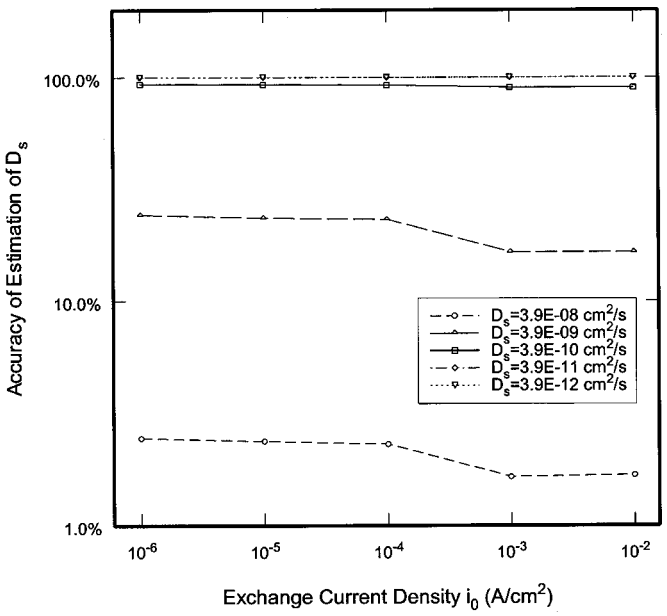

Figure 6. The accuracy of estimation of D_s with different parameter values of the exchange current density (all the other unmentioned parameters keep their base value).

estimation by the modified EIS method is insensitive to the relative size of two conductivity parameters of both phases.

Figure 6 reveals approximately similar phenomena to the above one. The estimation by the modified EIS method is insensitive to the magnitude of exchange current for the case studied here. This information seems to be helpful since knowing the exact kinetics parameter value is not required in order to get a valid estimation of D_s.

Figure 7 shows that, except for very small true values of D_s, the estimation accuracy tends to decrease as the radius of carbon particle decreases. We can explain this result by noting that the decrease of particle size not only facilitate the diffusion of lithium inside the solid particle (shorter diffusion path) but also increases the surface area of the electrode. All these lead to the increased reaction capability on the particle surface, which has the similar effect to that of having a larger exchange current density i_0 in Newman's dimensionless group 42. On the other hand, bigger particle size favors improved accuracy of the estimation of D_s.

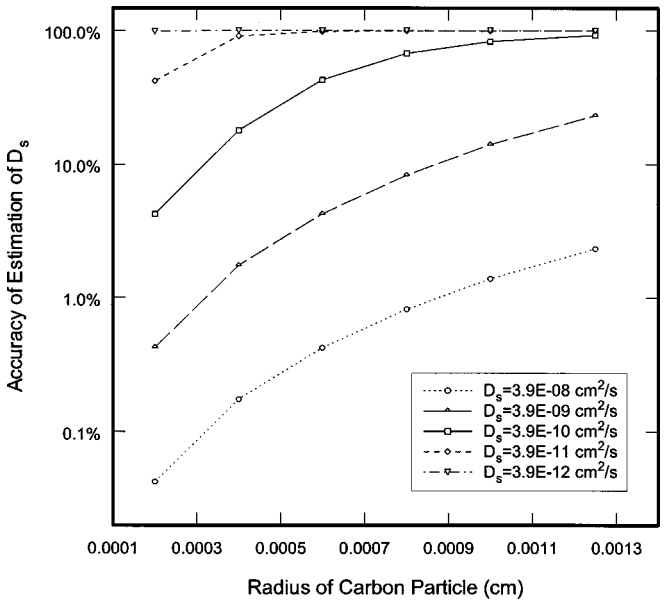

Figure 7. The accuracy of estimation of D_s with different carbon particle size (all the other unmentioned parameters keep their base values).

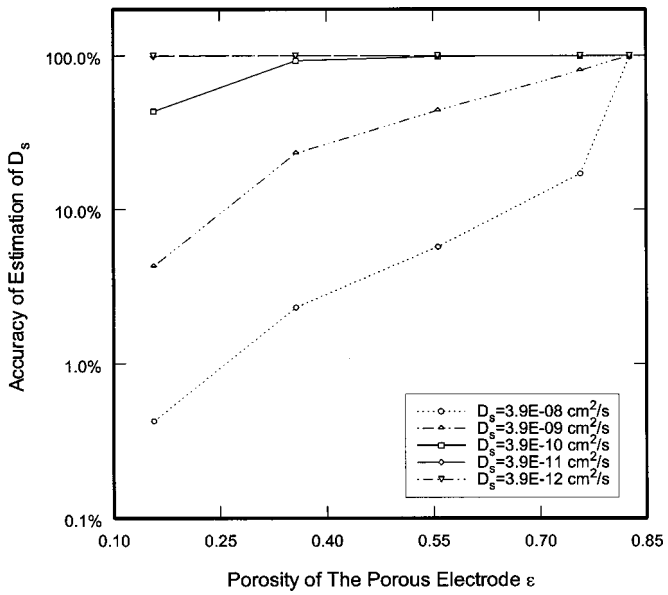

Figure 8. The accuracy of estimation of D_s with different parameter values of electrode (all the other unmentioned parameters keep their base values).

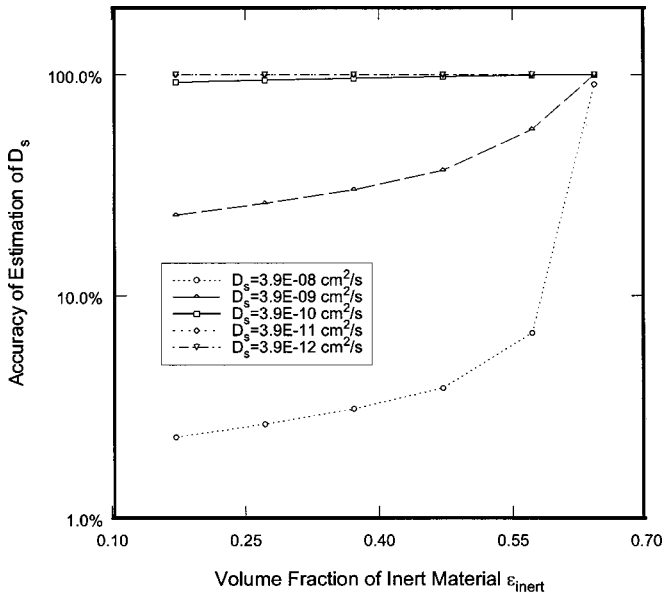

Figure 9. The accuracy of estimation of D_s with different parameter values of the volume fraction of inert material (all the other parameters keep their base values).

The significance of the change of the porous electrode porosity to the validity of D_s estimation is revealed in Fig. 8. For each curve, which corresponds to a fixed true value of D_s, the estimation becomes better as the porosity ε increases. When porosity reaches such a value that the summation of porosity and the volume fraction of invert material ε_{inert} approaches unity, the estimation is good even for large true values of D_s. The volume fraction of inert material plays a similar role on the validity of D_s estimation, which is demonstrated in Fig. 9. The above two results seem to be encouraging

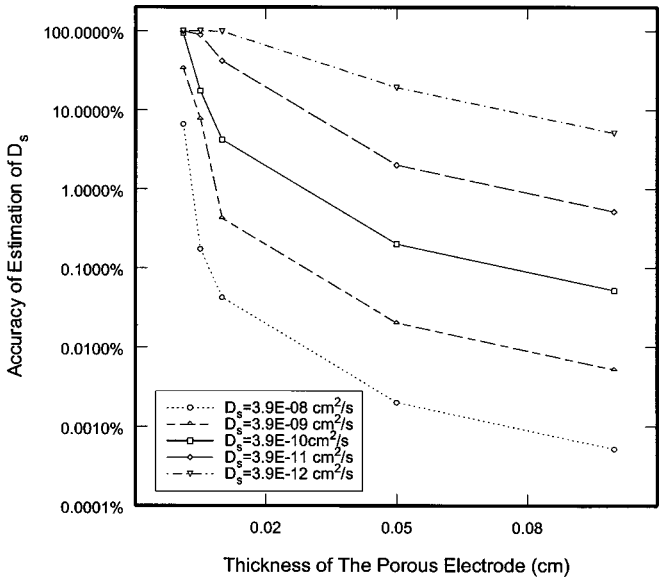

Figure 10. The accuracy of estimation of D_s with different parameter values of the electrode thickness (all the other parameters keep their base values).

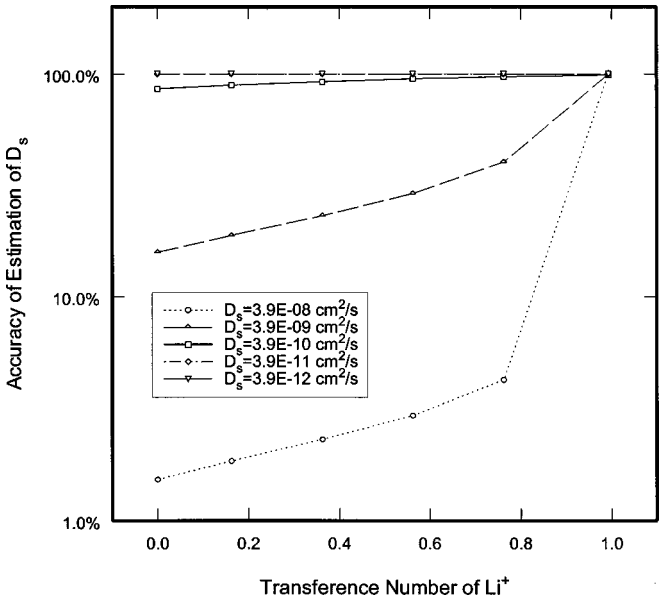

Figure 12. The accuracy of estimation of D_s with different values of lithium-ion transference number (all the other parameters keep their base values).

since we might be able to get a good estimation of D_s if we try to make the summation of ε and ε_{inert} approach 1. However, a small amount of loading of active material-carbon particles is required in either case. The mechanical strength of the porous electrode could be a problem if we increase the porosity so much, and the inert material could be not completely inert to lithium intercalation if we increase the volume fraction of this parameter. These things must be taken into account when we prepare electrode for impedance measurement in the lab.

The effect of different electrode thickness on the accuracy of estimation of D_s is studied by, first, changing the base value of carbon particle radius to 2 μm. Then the validity of estimation of D_s is investigated for the electrode thickness δ ranging from 10 to 1000 μm. As we can see from Fig. 10, the accuracy of D_s estimation increases as δ decreases. Since large particle size favors a good estimation of D_s, as is already shown in Fig. 7, a further improvement of estimation might be possible if we hold the particle size to the base value and decrease the electrode thickness to a very small value, such as 50 μm. However, attention must be paid in this case to check if we can use safely the macroscopic model, since the local average quantities might be inappropriate if the electrode thickness is not large compared to the active material particles.[18]

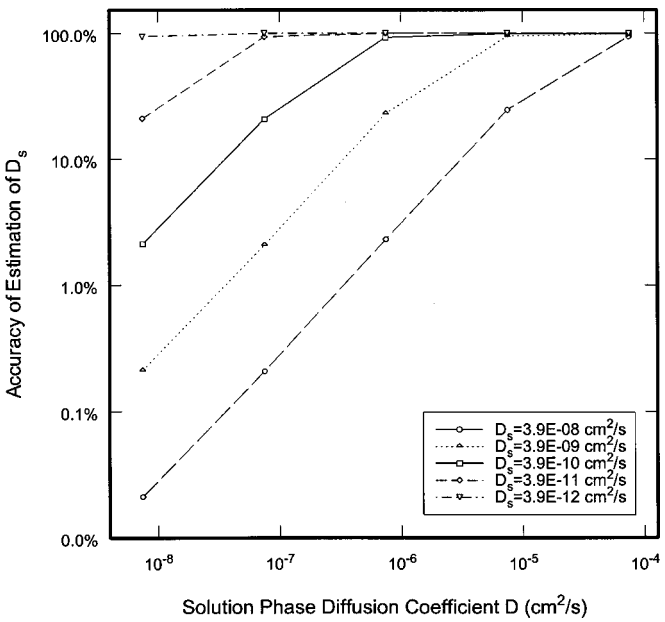

Figure 11. The accuracy of estimation of D_s with different parameter values of the solution phase diffusion coefficient (all the other parameters keep their base values).

The importance of the solution phase transport of lithium ion to the porous electrode is shown in Fig. 11 and Fig. 12. When the parameter value of solution phase diffusion coefficient is very large, such as 7.5×10^{-5} cm^2/s, the accuracy of D_s estimation is good for all the true values of D_s ranging from 3.9×10^{-12} to 3.9×10^{-8} cm^2/s. This is demonstrated in Fig. 11. When the value of the solution phase diffusion coefficient decreases, valid estimation of D_s exists only for very small true value of it. From this result, we may suspect that the limited ability of solution phase transport is responsible for the nonlinear reaction current distribution inside the porous electrode and, as a consequence, the bad estimation of D_s.

Further evidence is given in Fig. 12, where the estimation accuracy for all the true values of D_s is high when the transference number of lithium ion is close to 1. In this case, the solution phase concentration of lithium ion is actually uniform inside the porous electrode because the solution phase diffusion resistance is absent. Under the condition where there is no solution phase transport limitation, the estimation of D_s seems to be always good.

To summarize the above results, let us consider a dimensionless group 44, which can be understood as the ratio of two time constants for solid phase diffusion and solution phase diffusion. The accuracy of estimation as a function of this time constant ratio is plotted in Fig. 13. As we can see, when the ratio of two time constants is smaller than 0.001, the estimation is completely bad; when this ratio is larger than 1.0, the estimation is very good. This dimensionless group can help us evaluate the optimal experimental conditions in the lab for a reliable estimation of D_s from impedance spectrometry

$$\frac{\tau_s}{\tau_e} = \frac{R_s^2/a\delta D_s}{\delta^2/\varepsilon D_{eff}} = \frac{D}{D_s}\frac{R_s^3}{\delta^3}\frac{\varepsilon^{1.5}}{3(1-\varepsilon-\varepsilon_{inert})} \qquad [44]$$

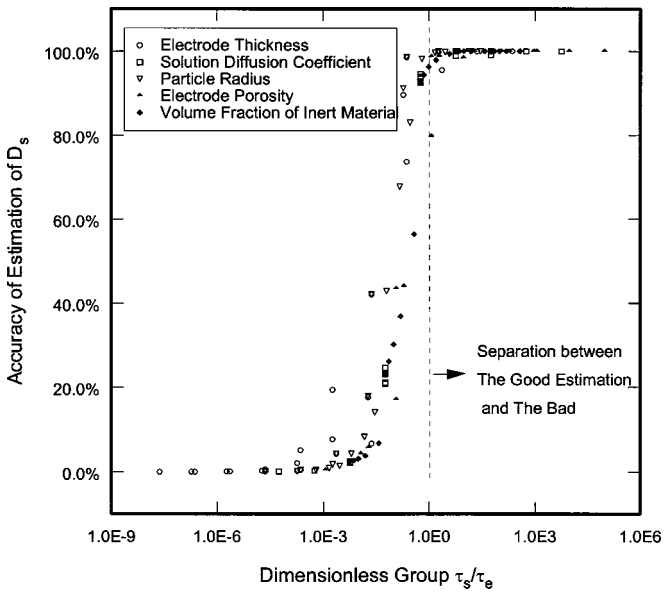

Figure 13. The accuracy of estimation of D_s as a function of the ratio of two time constants (reinterpretation of the results of Fig. 7, 8, 9, and 10).

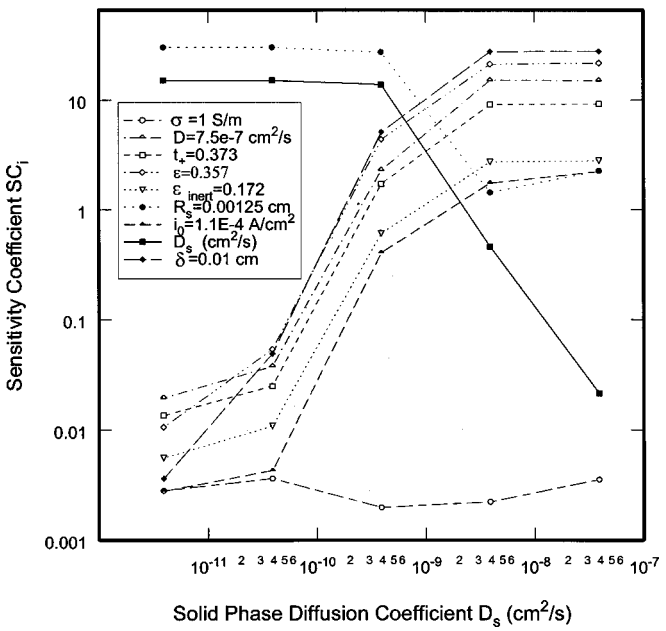

Figure 14. The sensitivity analysis of the impedance gradient in the transition region to the change of different parameter values (all the other unmentioned parameters keep their base values).

Unfortunately, the dimensionless group was seldom made larger than 1.0 in literature. For example, in the work of Yu *et al.*,[6] an estimation of D_s for graphite was extracted to be 1.12×10^{-10} and 6.51×10^{-11} cm^2/s for 0 and 30% state-of-charge (SOC) at 25°C. Since the particle size was quite small, around 1.5 μm in diam, and the working electrode had the thickness of 95 μm, a rough value of 0.0006-0.001 of the dimensionless time constant ratio is calculated, assuming the solution phase diffusion coefficient to be 7.5×10^{-7} cm^2/s, the porosity to be 0.4 and the volume fraction of inert material to be 0.1. This reminds us that their estimation might involve large error if all the assuming parameter values were appropriate. As another example, consider a $LiTiS_2$ electrode discussed by Doyle *et al.*[12] When the true value of D_s is smaller than 1×10^{-13} cm^2/s in Table II of their work, they had a reasonable estimation with the use of traditional Warburg approach. The dimensionless group for this value equals 1.0, which agrees with our result from the carbon electrode that a valid estimation of D_s is possible under this condition.

Since the modified EIS method cannot give us a reliable estimation if the dimensionless group is much less than 1.0, a "full model" method is developed as a strategy to address such situation.

Numerical parameter estimation by a full model.—By full model we mean we apply the same form of model equations Eq. 24-33, as are also used for the generation of simulated impedance data, for the estimation of D_s. This method is expected to work very well when we know the values for all the other parameters exactly. However, some parameters are very hard to be known with high accuracy, such as the exchange current density. Therefore, it is desired that we are still able to get a good estimation of D_s when the values of some other parameters are not assigned correctly. As an analogy to the modified EIS method, the gradient in the transition region is chosen to be the objective function here. We can write the gradient of Nyquist plot as an implicit function 45 of frequency and all the parameters

$$\frac{dZ_{\mathrm{Im}}}{dZ_{\mathrm{Re}}} = f(\omega, D_s, D, i_0, t_+^0, \delta, \ldots) \qquad [45]$$

Basically, a similar nonlinear parameter estimation technique to the one discussed above is also used here to get D_s back except that we have to resort to the numerical calculation for each element of the Jacobian matrix Eq. 46

$$J_{i,1} = \frac{\left(\frac{dZ_{\mathrm{Im}}}{dZ_{\mathrm{Re}}}\right)_{D_s+\Delta D_s} - \left(\frac{dZ_{\mathrm{Im}}}{dZ_{\mathrm{Re}}}\right)_{D_s-\Delta D_s}}{2\Delta D_s} \qquad [46]$$

where $J_{i,1}$ refers to the ith element of the one-dimensional matrix.

As is the case for the modified EIS method, we expect that some of the parameters in the full model might not be important and would not require the exact knowledge of the their values. Thus, it is important to determine the sensitivity of the model predictions to changes in the model parameters. If the model predictions are relatively insensitive to one or more of the parameters, then a fairly wide range of values for these insensitive parameters could be used without significantly affecting the predictions of the model. The sensitivity of the model predictions to changes in parameters is determined here by monitoring the change in the gradient of the Nyquist impedance curve. While holding all the other parameters constant, the parameter of interest is perturbed slightly and the resulting change in impedance gradient ranging from −4.0 to −12.0 is noted. We can find the sensitivity coefficient, SC_i, of that parameter by Eq. 47, following the same formula adopted by Evans and White[19]

$$SC_i = \frac{\sum_{j=1}^{n} \left| \Delta\left(\frac{dZ_{\mathrm{Im}}}{dZ_{\mathrm{Re}}}\right)_j \right|}{n|\Delta P_i|} \qquad [47]$$

where

$$\Delta\left(\frac{dZ_{\mathrm{Im}}}{dZ_{\mathrm{Re}}}\right)_j = \left(\frac{dZ_{\mathrm{Im}}}{dZ_{\mathrm{Re}}}\right)_j - \left(\frac{dZ_{\mathrm{Im}}}{dZ_{\mathrm{Re}}}\right)_j^* \qquad [48]$$

and

$$\Delta P_i = \frac{P_i - P_i^*}{P_i^*} \qquad [49]$$

Table III. Comparison of estimation results of D_s with 95% confidence intervals between the modified EIS method and the full model method (all the other parameters are assigned their base values).

True value of D_s put in simulation	Estimation of D_s by full model method	Estimation of D_s by modified EIS method
3.9×10^{-08} cm^2/s	$(4.22 \pm 0.33) \times 10^{-08}$ cm^2/s	$(9.00 \pm 0.04) \times 10^{-10}$ cm^2/s
3.9×10^{-09} cm^2/s	$(3.80 \pm 0.13) \times 10^{-09}$ cm^2/s	$(9.02 \pm 0.03) \times 10^{-10}$ cm^2/s
3.9×10^{-10} cm^2/s	$(3.90 \pm 0.01) \times 10^{-10}$ cm^2/s	$(3.60 \pm 0.01) \times 10^{-10}$ cm^2/s
3.9×10^{-11} cm^2/s	$(3.90 \pm 0.01) \times 10^{-11}$ cm^2/s	$(3.90 \pm 0.01) \times 10^{-11}$ cm^2/s
3.9×10^{-12} cm^2/s	$(3.90 \pm 0.01) \times 10^{-12}$ cm^{-2}/s	$(3.90 \pm 0.01) \times 10^{-12}$ cm^2/s

where P_i and P_i^* are the perturbed value and the reference value of parameter i, respectively. $(dZ_{Im}/dZ_{Re})_j$ is the value of the impedance gradient when using P_i, and $(dZ_{Im}/dZ_{Re})_j^*$ is the value when using P_i^*. Finally, n is the number of data points over which the gradients are compared.

Figure 14 gives the sensitivity of the impedance gradient to all the parameters that are important to the estimation of D_s over a range of true values of D_s. In this figure, all the other parameters except D_s and the parameter of interest are held at their base values. As is shown, when the true value of D_s is very small, *i.e.*, less than 3.9×10^{-10} cm^2/s, only the particle size R_s and D_s are important. This agrees with the modified EIS method that has no requirement of knowing all the other parameter values except R_s and D_s. However, when the true value of D_s is larger than 3.9×10^{-10} cm^2/s, all the other parameters such as the exchange current density i_0, solid phase conductivity σ, porosity ε, volume fraction of inert material ε_{inert}, active material particle size R_s, thickness δ and solution phase diffusion coefficient D are also important and effect the impedance response. The impedance gradient becomes more insensitive to the change of solid phase diffusion coefficient D_s as the true value of this becomes bigger. This warns us that an exact knowledge of the values for all the possible parameters is needed for the estimation of D_s for high true values of D_s. It can also be seen from Fig. 14 that the solid phase conductivity always plays an insignificant role.

The impedance data we collect in the lab usually involve error or noise, the origin of which might not be clear. In this work, we also include some random noise to the synthetic impedance gradient data calculated from the simulation. A random error generator by Maple VI was used to produce a group of normally distributed error, ϕ, with mean zero and variance one [*i.e.*, $\sim N$ (0, 1)]. This error is added to the synthetic gradient data ranging from -4.0 to -12.0 by

$$\left(\frac{dZ_{Im}}{dZ_{Re}}\right)_{j,\text{with error}} = \left(\frac{dZ_{Im}}{dZ_{Re}}\right)_j + 0.05\phi \quad [50]$$

As was stated by Evans and White,[19] an estimate of a parameter has little meaning unless it is accompanied by some approximation of the possible error it possesses. Therefore, a confidence interval is needed to obtain together with the estimation. It can be calculated by the following expression

$$P_i = \hat{P}_i + t_{(1-\gamma/2),(n-m)} S_{P_i} \quad [51]$$

where $\hat{P}_i$ is the estimate of parameter P_i, $t_{(1-\gamma/2),(n-m)}$ is the student t-distribution at $(1 - \gamma/2) \times 100\%$ confidence level, n is the number of observations, m is the number of parameters, $n - m$ is the degree of freedom, and S_{P_i} is the estimate of the variance for P_i, which is calculated from mean square error, S_E^2, by

$$S_{P_i} = \sqrt{(J^T J)^{-1} S_E^2} \quad [52]$$

where **J** is the Jacobian matrix (see Eq. 46) and S_E^2 is calculated by

$$S_E^2 = \frac{\sum_{j=1}^{n} \left[\left(\frac{dZ_{Im}}{dZ_{Re}}\right)_{obs} - \left(\frac{dZ_{Im}}{dZ_{Re}}\right)_{pred} \right]^2}{n - m} \quad [53]$$

A comparison of the estimation results, between the full model method and the modified EIS method, from the same synthetic impedance data with noise is tabulated in Table III. All the other parameters except D_s are assumed to be known exactly to us before we apply the full model method to the estimation. As we can see, the full model does give reasonable estimations of D_s for all the true

Table IV. Comparison of estimation results of D_s with 95% confidence intervals between the modified EIS method and the full model method assuming one of the parameter values is not known correctly before estimation (all the other parameters are assigned their base values).

True value of D_s (cm^2/s) used in the impedance simulation	Estimation of D_s (cm^2/s) if $\sigma = 0.001$ S/cm	Estimation of D_s (cm^2/s) if $\sigma = 0.01$ S/cm	Estimation of D_s (cm^2/s) if $i_0 = 1.1 \times 10^{-2}$ A/cm^2	Estimation of D_s (cm^2/s) if $i_0 = 1.1 \times 10^{-6}$ A/cm^2
3.9×10^{-08}	[a] $(2.71 \pm 0.46) \times 10^{-09}$	$(4.54 \pm 1.21) \times 10^{-09}$	Not Converge	$(3.90 \pm 0.01) \times 10^{-09}$
	[b] $(9.00 \pm 0.04) \times 10^{-10}$	$(9.00 \pm 0.04) \times 10^{-10}$	$(9.00 \pm 0.04) \times 10^{-10}$	$(9.00 \pm 0.04) \times 10^{-10}$
3.9×10^{-09}	[a] $(3.42 \pm 0.21) \times 10^{-09}$	$(2.23 \pm 0.22) \times 10^{-09}$	Not converge	$(1.03 \pm 0.32) \times 10^{-10}$
	[b] $(9.02 \pm 0.03) \times 10^{-10}$	$(9.02 \pm 0.03) \times 10^{-10}$	$(9.02 \pm 0.03) \times 10^{-10}$	$(9.02 \pm 0.03) \times 10^{-10}$
3.9×10^{-10}	[a] $(3.80 \pm 0.12) \times 10^{-10}$	$(3.88 \pm 0.09) \times 10^{-10}$	$(4.03 \pm 0.01) \times 10^{-10}$	$(3.80 \pm 0.01) \times 10^{-10}$
	[b] $(3.61 \pm 0.01) \times 10^{-10}$	$(3.61 \pm 0.01) \times 10^{-10}$	$(3.61 \pm 0.01) \times 10^{-10}$	$(3.61 \pm 0.01) \times 10^{-10}$
3.9×10^{-11}	[a] $(3.90 \pm 0.01) \times 10^{-11}$	$(3.90 \pm 0.01) \times 10^{-11}$	$(3.90 \pm 0.01) \times 10^{-11}$	$(3.90 \pm 0.01) \times 10^{-11}$
	[b] $(3.90 \pm 0.01) \times 11^{-11}$	$(3.90 \pm 0.01) \times 10^{-11}$	$(3.90 \pm 0.01) \times 10^{-11}$	$(3.90 \pm 0.01) \times 10^{-11}$
3.9×10^{-12}	[a] $(3.90 \pm 0.01) \times 10^{-12}$	$(3.90 \pm 0.01) \times 10^{-12}$	$(3.90 \pm 0.01) \times 10^{-12}$	$(3.90 \pm 0.01) \times 10^{-12}$
	[b] $(3.90 \pm 0.01) \times 10^{-12}$	$(3.90 \pm 0.01) \times 10^{-12}$	$(3.90 \pm 0.01) \times 10^{-12}$	$(3.90 \pm 0.01) \times 10^{-12}$

[a] Estimation by the full model method.
[b] Estimation by the modified EIS method.

values of this parameter, with the expected true value lying between the confidence intervals. However, one should also notice that the confidence intervals for larger true values of D_s are large compared to those for smaller true values. This can be explained by that the impedance gradient is not sensitive to the change of solid phase diffusion coefficient at higher true values of them, compared with other parameters, if we look at Fig. 14. A small noise might produce much deviation from the expected estimation. When the true value of D_s is smaller than 3.9×10^{-10} cm^2/s, both methods are equally accurate because the impedance gradient is very sensitive to the change of solid phase diffusion coefficient.

As explained before, we might expect that the full model method does not require knowing exactly some of the parameters, such as solid phase conductivity, exchange current density, etc. To check this, we use the same synthetic impedance data as those used for the case in Table III. Then we assume that one of the parameters, such as the exchange current density and solid phase conductivity, is not known correctly. After this, we find the estimation of D_s by assigning different values of this parameter. The results are shown in Table IV. We observe that the two methods agree with each other when the expected true value of D_s is small, *i.e.*, less than 3.9×10^{-10} cm^2/s in this case. We also observe that inaccurate knowledge of the values for such parameters as the exchange current density and solid phase conductivity leads to large estimation error if the true value of D_s is large, where the solid phase diffusion is not the dominant process. We can suspect from this that exactly knowing the values for all the parameters discussed in this work is required if we want to use the full model to get a reliable estimation of D_s from the impedance response where the modified EIS method becomes bad.

Conclusion

We conclude from above discussion that the validity of estimating D_s from the impedance response of a porous intercalation electrode by the modified EIS method is not assured if we have limited capability of transport of lithium ion of the solution phase in the porous intercalation electrode. A dimensionless group, the ratio of time constant of solid phase diffusion τ_s and that of solution phase diffusion τ_e, is useful to evaluate the experimental conditions by using this method for a reliable estimation of D_s from a porous electrode. Big particle radius, small electrode thickness, large difference of the true parameter value of D and D_s, and small active material loading are conducive to a valid estimation of solid phase diffusion coefficient.

For the case where the modified EIS method works poorly, a full model method is provided here. However, exactly knowing the values of all the other parameters is required in order to get a valid estimation.

Acknowledgments

The authors are grateful for the financial support of the project by National Reconnaissance Organization (NRO) under contract no. 1999 I016400 000 000.

The University of South Carolina assisted in meeting the publication costs of this article.

Appendix

$$\tilde{j}_{n,f,Re} = \left(\frac{i_0}{RT} - \frac{W_5}{W_6}\right)(\tilde{\Phi}_{1,Re} - \tilde{\Phi}_{2,Re}) - \frac{W_7}{W_6}(\tilde{\Phi}_{1,Im} - \tilde{\Phi}_{2,Im}) \quad [A\text{-}1]$$

$$\tilde{j}_{n,f,Im} = \left(\frac{i_0}{RT} - \frac{W_5}{W_6}\right)(\tilde{\Phi}_{1,Im} - \tilde{\Phi}_{2,Im}) + \frac{W_7}{W_6}(\tilde{\Phi}_{1,Re} - \tilde{\Phi}_{2,Re}) \quad [A\text{-}2]$$

where

$$W_5 = \frac{{i_0}^2 R_s}{RT}\frac{dU}{dc_s}\bigg|_{c_s=c_{s,0}}\left[i_0\frac{dU}{dc_s}\bigg|_{c_s=c_{s,0}} R_s + D_s RT - R_s\frac{W_1}{W_4}(W_2 + W_3)\right] \quad [A\text{-}3]$$

$$W_6 = \left[i_0 R_s\frac{dU}{dc_s}\bigg|_{c_s=c_{s,0}} + D_s RT - R_s\frac{W_1}{W_4}(W_2 - W_3)\right]^2 + R_s^2\frac{W_1^2}{W_2^2}(W_3 - W_2)^2 \quad [A\text{-}4]$$

$$W_4 = \sinh\left(R_s\sqrt{\frac{\omega}{2D_s}}\right)^2 + \sin\left(R_s\sqrt{\frac{\omega}{2D_s}}\right)^2 \quad [A\text{-}5]$$

$$W_3 = \sin\left(R_s\sqrt{\frac{\omega}{2D_s}}\right)\cos\left(R_s\sqrt{\frac{\omega}{2D_s}}\right) \quad [A\text{-}6]$$

$$W_2 = \sinh\left(R_s\sqrt{\frac{\omega}{2D_s}}\right)\cosh\left(R_s\sqrt{\frac{\omega}{2D_s}}\right) \quad [A\text{-}7]$$

$$W_1 = RT\sqrt{\frac{D_s\omega}{2}} \quad [A\text{-}8]$$

List of Symbols

a	effective specific surface area of the porous electrode, cm^{-1}
A	effective surface area per unit mass of the electrode, cm^2/g
c	concentration of lithium ion in the solution phase, mol/cm^3
c_0	concentration of lithium ion under open-circuit condition, mol/cm^3
$\tilde{c}_{Re}$	real part of the deviation concentration of lithium ion in the solution phase in Laplace domain, mol/cm^3
$\tilde{c}_{Im}$	imaginary part of the deviation concentration of lithium ion in the solution phase in Laplace domain, mol/cm^3
c_s	concentration of lithium on the solid carbon particle, mol/cm^3
$c_{s,0}$	concentration of lithium in the solid carbon particle under open-circuit condition, mol/cm^3
C_{dl}	double-layer capacitance of the porous electrode, F/cm^2
$C_{dl,c}$	double-layer capacitance of the counter electrode, F/cm^2
D	diffusion coefficient of the bulk solution phase, cm^2/s
D_{eff}	effective diffusion coefficient of the solution phase, $D_{eff} = D \times \varepsilon^{0.5}$ for the porous electrode and $D_{eff} = D \times \varepsilon_s^{0.5}$ for the separator, cm^2/s
D_s	solid phase diffusion coefficient of lithium inside the carbon particle, cm^2/s
$f_{\pm,0}$	mean activity coefficient of the lithium salt in the solution phase under open-circuit condition
$f'_{\pm,0}$	derivative of the mean activity coefficient of lithium salt in the solution phase under open-circuit condition
F	Faraday's constant, 96487 C/mol
I	total current density applied to the T-cell, A/cm^2
i_0	exchange current density of carbon electrode, A/cm^2
$i_{0,c}$	exchange current density of the counter electrode, A/cm^2
i_2	current density in the solution phase, A/cm^2
$j_{n,f}$	pore-wall flux across interface, mol/cm^2-s
J	specific current per unit mass of active material, A/g
M	total number of node points used for the T-cell
N	total number of node points used for the working electrode
R	gas constant, 8.3143J/mol K
R_s	radius of the carbon particle, cm
SC_i	the sensitivity coefficient of the impedance gradient in the transition region to the change of parameter i
t_+^0	transference number of lithium ion in the solution phase
t_-^0	transference number of anion in the solution phase
T	ambient temperature under study, 298.15 K
U	equilibrium potential of the carbon electrode at local concentration, V
V_m	molar volume of the lithiated material, cm^3/mol
x	coordinate of the cell, cm
Z_{Re}	real component of the complex impedance, Ω cm^2
Z_{Im}	imaginary component of the complex impedance, Ω cm^2

Greek

δ	thickness of the working electrode, cm
δ_s	thickness of the separator, cm
ε	porosity of the porous electrode
ε_{inert}	volume fraction of inert material of the porous electrode
ε_s	porosity of the separator
κ	conductivity of the bulk solution phase, S/cm
κ_{eff}	effective conductivity of the solution phase, $\kappa_{eff} = \kappa \times \varepsilon^{1.5}$ for the working electrode, and $\kappa_{eff} = \kappa \times \varepsilon_s^{1.5}$ for the separator, S/cm
σ	Bulk solid phase conductivity, S/cm
σ_{eff}	effective conductivity of the solid phase, $\sigma_{eff} = \sigma \times (1 - \varepsilon)^{1.5}$, S/cm
τ_s	time constant for solid phase diffusion of Li, s^{-1}
τ_e	time constant for solution phase diffusion of Li$^+$, s^{-1}
Φ_1	solid phase potential, V
$\tilde{\Phi}_{1,Re}$	real part of the deviation of solid phase potential in Laplace domain, V
$\tilde{\Phi}_{1,Im}$	imaginary part of the deviation of solid phase potential in Laplace domain, V
Φ_2	solution phase potential, V

$\tilde{\Phi}_{2,\mathrm{Re}}$ real part of the deviation of solution phase potential in Laplace domain, V
$\tilde{\Phi}_{2,\mathrm{Im}}$ imaginary part of the deviation of solution phase potential in Laplace domain, V
ω angular frequency, rad/s

Subscripts

$+$ to the right of an interface
$-$ to the left of an interface

Superscripts

T transpose of a matrix
-1 the inverse of a matrix

References

1. J. F. Fauvarque, S. Guinot, N. Bouzir, E. Salmon, and J. F. Penneau, *Electrochim. Acta*, **40**, 2449 (1995).
2. S. Guinot, E. Salmon, J. F. Penneau, and J. F. Fauvarque, *Electrochim. Acta*, **43**, 1163 (1998).
3. S. Guinot, N. Bouzir, J. F. Penneau, and J. F. Fauvarque, in *Rechargeable Zinc Batteries*, A. J. Salkind, F. R. McLarnon, and V. S. Bagotsky, Editors, PV 95-14, p. 182, The Electrochemical Society Proceedings Series, Pennington, NJ (1995).
4. M. Oshitani, H. Yufu, K. Takashima, S. Tsuli, and Y. Matsumaru, *J. Electrochem. Soc.*, **136**, 1590 (1989).
5. H. Ogawa, M. Ikoma, H. Kawano, and I. Matsumoto, *J. Power Sources*, **12**, 393 (1989).
6. Ping Yu, B. N. Popov, J. A. Ritter, and R. E. White, *J. Electrochem. Soc.*, **146**, 8 (1999).
7. B. S. Haran, B. N. Popov, and R. E. White, *J. Power Sources*, **75**, 56 (1998).
8. S. Motupally, C. C. Streinz, and J. W. Weidner, *J. Electrochem. Soc.*, **142**, 1401 (1995).
9. M. W. Verbrugge and B. J. Koch, *J. Electrochem. Soc.*, **146**, 833 (1999).
10. W. Weppner and R. A. Huggins, *J. Electrochem. Soc.*, **124**, 1569 (1977).
11. C. J. Wen, B. A. Boukamp, and R. A. Huggins, *J. Electrochem. Soc.*, **126**, 2258 (1979).
12. M. Doyle, J. P. Meyers, and J. Newman, *J. Electrochem. Soc.*, **147**, 99 (2000).
13. R. E. Meredith and C. W. Tobias, in *Advances in Electrochemical Engineering*, C. W. Tobias, Editor, Vol. 2, p. 15, Interscience Publishers, New York (1962).
14. M. Doyle and J. Newman, *J. Electrochem. Soc.*, **143**, 1890 (1996).
15. V. R. Subramanian and R. E. White, *Chem. Eng. Educ.*, **34**, 328 (2000).
16. A. Constantinides, *Numerical Methods for Chemical Engineers with MATLAB Applications*, p. 490, Prentice Hall, New Jersey (1999).
17. J. S. Newman, *Electrochemical Systems*, 2nd ed., p. 462, Prentice Hall, New Jersey (1991).
18. J. C. Slattery, *Advanced Transport Phenomena*, p. 573, Cambridge University Press, New Jersey (1999).
19. T. I. Evans and R. E. White, *J. Electrochem. Soc.*, **136**, 2798 (1989).